International Journal of Thermophysics, Vol. 6, No. 2, 1985

Thermal Conductivity of Methane for Temperatures Between 110 and 310 K with Pressures to 70 MPa

H. M. Roder[1]

Received July 12, 1984

The paper presents new experimental measurements of the thermal conductivity of methane for 14 temperatures between 110 and 310 K with pressures to 70 MPa and densities from 0 to 30 mol · L^{-1}. The measurements were made with a transient hot-wire apparatus and they cover a wide range of physical states including the dilute gas, the moderately dense gas, the near-critical region, the compressed liquid states, and the vapor at temperatures below the critical temperature. The new measurements are closely spaced in temperature and density to describe the thermal conductivity surface, in particular the critical enhancement which extends to the highest temperature measured. A fit of the thermal conductivity surface allows comparison of the present results to those of others. The comparison reveals several discrepancies inherent in the results of others and in an earlier correlation. The precision (2σ) of the methane measurements is between 0.5 on 0.8% for wire temperature transients of 4 to 5 K, while the accuracy is estimated to be 1.6%.

KEY WORDS: density; high pressure; hot wire; methane; thermal conductivity; transient measurements.

1. INTRODUCTION

A search of the literature reveals a relative abundance of papers on the thermal conductivity of methane. Several of these papers cover a wide range in both temperature and density [1–3], and at least one is devoted to a critical evaluation and correlation of the entire thermal conductivity surface of methane [4]. In these circumstances it might seem presumptuous to offer yet another set of experimental data on methane.

[1] Chemical Engineering Science Division, National Bureau of Standards, Boulder, Colorado 80303, USA.

0195-928X/85/0300-0119$04.50/0

However, we were planning to measure the thermal conductivity of a series of methane–ethane mixtures. Before starting on the mixtures it seemed prudent first to measure the pure components in our apparatus, in order to establish a reliable and consistent base on which to build. In this paper new experimental measurements are presented that cover a large range in density for nearly every isotherm, i.e., 0 to 18 $mol \cdot L^{-1}$ for 310 K and 0 to 30 $mol \cdot L^{-1}$ for 135 K. The results are used to develop a new correlation for the thermal conductivity surface of methane for temperatures between 110 and 310 K and for pressures up to 70 MPa.

Analysis after the fact justified our decision to make new measurements, which were taken with a density spacing of roughly 1 $mol \cdot L^{-1}$. The new measurements are sufficiently precise and detailed to describe the fine structure of the thermal conductivity surface. In particular, the new measurements show the extent of the near-critical region enhancement which is till discernible at a temperature of 310 K. The present results agree to better than 1% with those of other authors [1–3] in some parts of the thermal conductivity surface, yet the comparison reveals clearly several deficiencies in the earlier papers. Similarly, the comparison of the present curve fit with the earlier critical evaluation [4] reveals several deficiencies. In view of the new measurements a revision of the earlier correlation is called for.

2. METHOD AND APPARATUS

The measurements were made with a transient hot-wire thermal conductivity apparatus. This instrument has been tested with nitrogen [5], helium [5], and argon [6, 7]. It has been used to measure the thermal conductivity surfaces of oxygen [8], propane [9], and hydrogen [10]. Detailed descriptions of the apparatus, of the experimental procedure, of the wire calibration, of the data reduction, and of the apparatus performance are given in the apparatus paper [5]. Two changes initially adopted for the measurements on oxygen [8] were retained: a digital filter was applied to the voltages measured across the bridge, and the deviation plot of experimental temperature rises is now linear. New wires had been mounted during the measurements on hydrogen. For the new wires a cubic equation in temperature is used to represent the wire calibration. The methane measurements fall into two of the three series described in Ref. 10. Isotherms at 310, 275, 255, and 232 K were measured with the wires calibrated in the "as received" state; all other isotherms, with the wires calibrated in the "partially annealed" state.

The samples used are research-grade methane stated by the supplier to be a minimum of 99.99 mol% methane. Chromatographic analysis of the

methane used showed no detectable impurities [11]. We used a small diaphragm compressor as a pressure intensifier and observed normal precautions for high pressure and high vacuum.

3. RESULTS

To define the thermal conductivity surface of methane, a grand total of 910 points was measured. A total of 8 points at temperatures and densities below critical was rejected because the experimental density was too high, i.e., condensation of sample on the wire occurred. Two additional points were rejected because of inadequate thermal equilibrium. The remaining 900 points are distributed among 14 isotherms as shown in Table I. The fluid states measured in this experiment include the dilute gas, dense gas, near-critical states, vapor at temperatures below critical, compressed liquid states, and metastable liquid states at densities below saturation. On each isotherm measurements were made at a number of different pressures. In the compressed liquid at the lower temperatures the spacing was about 11 MPa (1600 psia) in pressure. In the single-phase fluid the spacing in pressure was arranged to give a spacing in density of about 1 $mol \cdot L^{-1}$. At each pressure four different power levels are applied to the hot wire, resulting in slightly different experimental temperatures and densities.

For any given experimental point the pressure, cell temperature, and applied power are measured directly. The experimental temperature and

Table I. Distribution of the Experimental Measurements

Nominal temperature (K)	Vapor	Single phase	Compressed liquid
110			28
135	4		28
145	8		
155	12		32
165	12		
175	16		44
185	20		
197		105	
215		104	
235		96	
255		95	
275		100	
295		96	
310		100	

the thermal conductivity with its associated regression error are obtained through the data reduction program, while the density is calculated from an equation of state [12] using the measured pressure and the experimental temperature. We note that the experimental temperatures vary with the applied power and are several degrees higher than the cell temperature.

An overview of the thermal conductivities is given in Fig. 1, where the lines are the isotherms calculated from the correlation. A complete table

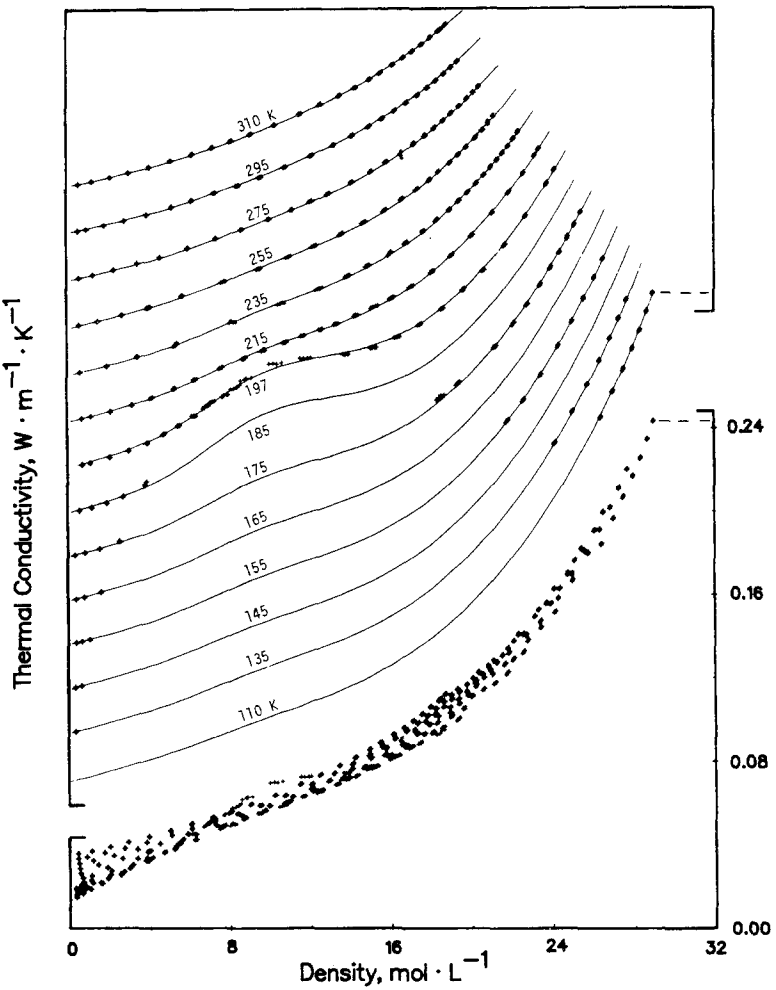

Fig. 1. Overview of the thermal conductivity measurements on methane. Bottom: all measurements on a single scale. Top: individual isotherms separated by 0.02 $W \cdot m^{-1} \cdot K^{-1}$.

which includes all 900 experimental measurements is given in Ref. 13. A summary of the experimental thermal conductivity values is presented in Table II, where, to conserve space, replicate measurements at any given pressure level are averaged to yield a single point. The 900 measurements were thus reduced to 250 points. In Table II the temperature, densities, and "experimental" thermal conductivities are averages of four measurements at different power levels. The pressures are calculated from the equation of state for the averaged density and temperature. The deviation of the experimental thermal conductivity from the new correlating equations (Section 4.4) is given in the next to last column in Table II. In much of the subsequent analysis it is desirable to have the thermal conductivities at integral values of temperature. Therefore, each point is adjusted at constant density to the nominal isotherm temperature by a slight shift in temperature using the correlating equation given in Section 4.4. The last column in Table II displays the thermal conductivity adjusted to an integral value of temperature.

The apparatus is not specifically designed to measure thermal conductivity in the critical region. Nevertheless, measurements were made as close to critical as is possible with the present system, bearing in mind that the measurements must be free of convention. The replicate measurements at the same cell temperature and pressure with different power levels serve to verify the absence of convection. The procedure changes the temperature rise in the wire and, hence, the temperature rise in the gas near the wire. The technique is quite analogous to changing the ΔT for a steady-state parallel plate system. Extensive comparisons of the effect of varying the power level for the transient hot-wire system were given for N_2 and He in the apparatus paper (Figs. 12 and 15 in Ref. 5) and for argon in Table II of Ref. 6. We conclude that the present measurements are free of convection.

4. CORRELATION OF THE THERMAL CONDUCTIVITY SURFACE

The features of the thermal conductivity surface of methane are quite similar to those of oxygen [8], therefore, the correlation of the methane surface follows the procedure outlined for oxygen. It is generally accepted that the thermal conductivity should be correlated in terms of density and temperature [14] rather than temperature and pressure, because over a wide range of experimental conditions the behavior of thermal conductivity is dominated by its density dependence. This preferred technique requires an equation of state [12] to translate measured pressures into equivalent

Table II. The Thermal Conductivity of Methane

Pressure (MPa)	Temperature (K)	Density ($mol \cdot L^{-1}$)	Thermal conductivities: Experimental ($W \cdot m^{-1} \cdot K^{-1}$)	Exp. − corr. (%)	At nom. T ($W \cdot m^{-1} \cdot K^{-1}$)
		Nom. temp. 110			
0.553	111.430	26.387	0.1847	−0.6	0.1843
11.637	111.331	26.986	0.1972	−0.2	0.1967
22.691	111.483	27.482	0.2077	−0.2	0.2072
34.113	111.328	27.943	0.2175	−0.3	0.2171
44.929	111.205	28.318	0.2262	−0.3	0.2257
56.736	111.081	28.669	0.2353	0.1	0.2348
68.644	110.962	28.973	0.2437	0.5	0.2528
		Nom. temp. 135			
0.315	133.874	0.304	0.0148	0.3	0.0149
0.764	134.867	24.096	0.1519	0.2	0.1519
11.709	134.906	24.922	0.1670	0.3	0.1670
22.962	134.752	25.727	0.1800	0.2	0.1800
34.177	134.872	26.313	0.1913	0.1	0.1913
45.576	134.713	26.838	0.2019	0.1	0.2020
56.748	134.823	27.265	0.2114	0.3	0.2115
67.926	134.643	27.654	0.2203	0.4	0.2232
		Nom. temp. 145			
0.357	144.330	0.316	0.0159	−0.6	0.0160
0.650	144.024	0.616	0.0166	−0.7	0.0178
		Nom. temp. 155			
0.429	153.922	0.357	0.0170	−0.9	0.0172
0.731	154.234	0.639	0.0177	−1.2	0.0178
1.082	153.919	1.022	0.0186	−1.1	0.0188
1.597	154.911	21.747	0.1227	0.1	0.1227
6.754	154.745	22.551	0.1327	−0.2	0.1327
14.577	154.976	23.391	0.1446	−0.2	0.1446
25.314	155.097	24.270	0.1584	−0.1	0.1584
35.994	155.214	24.961	0.1702	−0.1	0.1702

Table II. *(Continued)*

Pressure (MPa)	Temperature (K)	Density (mol·L^{-1})	Thermal conductivities: Experimental (W·m^{-1}·K^{-1})	Exp. − corr. (%)	At nom. T (W·m^{-1}·K^{-1})
46.630	155.063	25.554	0.1813	0.0	0.1813
56.924	154.875	26.051	0.1910	0.2	0.1911
67.033	154.708	26.478	0.1998	0.3	0.2021
		Nom. temp. 165			
0.446	164.385	0.344	0.0181	−1.3	0.0182
0.935	164.059	0.776	0.0190	−1.7	0.0192
1.657	163.617	1.592	0.0214	0.2	0.0228
		Nom. temp. 175			
0.406	174.541	0.292	0.0191	−1.2	0.0192
1.015	174.157	0.783	0.0202	−1.8	0.0203
1.751	173.754	1.512	0.0220	−1.4	0.0222
2.461	173.252	2.511	0.0256	2.3	0.0259
2.644	174.692	18.400	0.0942	2.2	0.0943
4.614	174.610	19.299	0.1006	0.9	0.1007
12.708	174.751	21.129	0.1180	−0.4	0.1180
19.722	174.995	22.055	0.1292	−0.5	0.1292
26.452	175.148	22.740	0.1383	−0.6	0.1383
33.796	175.004	23.375	0.1476	−0.4	0.1476
41.284	175.218	23.899	0.1559	−0.3	0.1559
48.146	175.099	24.340	0.1631	−0.3	0.1631
55.058	174.935	24.740	0.1703	−0.0	0.1703
61.639	174.834	25.084	0.1764	0.0	0.1765
68.370	175.000	25.391	0.1823	0.1	0.1840
		Nom. temp. 185			
0.752	184.665	0.523	0.0206	−2.5	0.0206
1.508	184.844	1.132	0.0220	−3.5	0.0220
2.252	184.439	1.870	0.0240	−3.2	0.0241
2.884	184.145	2.692	0.0270	−1.0	0.0272
3.450	183.857	3.791	0.0332	5.4	0.0345

Table II. *(Continued)*

Pressure (MPa)	Temperature (K)	Density ($mol \cdot L^{-1}$)	Thermal conductivities: Experimental ($W \cdot m^{-1} \cdot K^{-1}$)	Exp. − corr. (%)	At nom. T ($W \cdot m^{-1} \cdot K^{-1}$)
		Nom. temp. 197			
1.013	199.304	0.656	0.0227	−1.4	0.0224
1.531	198.607	1.038	0.0233	−2.7	0.0231
2.670	198.700	2.015	0.0259	−2.6	0.0258
3.520	198.365	2.964	0.0288	−2.4	0.0288
4.156	198.363	3.888	0.0325	−1.6	0.0326
4.569	198.100	4.711	0.0365	−0.7	0.0368
4.861	198.138	5.452	0.0405	−0.5	0.0409
5.049	197.697	6.210	0.0451	−0.7	0.0455
5.173	197.626	6.792	0.0493	0.3	0.0497
5.230	197.637	7.093	0.0515	0.8	0.0520
5.329	197.537	7.774	0.0546	−1.7	0.0552
5.408	197.640	8.271	0.0584	−0.3	0.0591
5.500	197.864	8.788	0.0622	1.6	0.0632
5.693	197.960	10.229	0.0694	3.2	0.0705
5.965	198.181	11.740	0.0720	1.5	0.0733
6.571	198.182	13.757	0.0741	−1.4	0.0750
7.445	198.136	15.132	0.0776	−1.7	0.0782
8.898	198.394	16.307	0.0827	−0.9	0.0831
11.179	198.758	17.422	0.0891	−0.4	0.0893
14.450	198.640	18.536	0.0968	−0.3	0.0969
19.219	199.026	19.573	0.1060	−0.1	0.1058
26.071	200.169	20.563	0.1151	−0.8	0.1148
35.264	200.430	21.616	0.1274	−0.7	0.1269
47.242	200.230	22.672	0.1413	−0.5	0.1409
62.619	200.558	23.676	0.1567	−0.0	0.1563
69.419	200.555	24.057	0.1635	0.4	0.1652
		Nom. temp. 215			
1.068	214.229	0.636	0.0243	−0.7	0.0244
1.747	214.546	1.083	0.0253	−1.1	0.0253
3.036	214.151	2.064	0.0276	−1.1	0.0277
4.165	213.843	3.125	0.0307	−0.6	0.0308
5.022	214.155	4.097	0.0341	0.4	0.0341
5.811	214.174	5.224	0.0385	0.9	0.0385
6.372	213.909	6.255	0.0428	0.7	0.0428
6.929	213.563	7.535	0.0485	−0.0	0.0483

Table II. *(Continued)*

Pressure (MPa)	Temperature (K)	Density ($mol \cdot L^{-1}$)	Thermal conductivities: Experimental ($W \cdot m^{-1} \cdot K^{-1}$)	Exp. − corr. (%)	At nom. T ($W \cdot m^{-1} \cdot K^{-1}$)
7.357	213.239	8.687	0.0533	−0.9	0.0531
7.760	213.342	9.659	0.0572	−0.9	0.0569
8.255	213.495	10.731	0.0609	−0.7	0.0606
8.697	213.436	11.606	0.0640	−0.2	0.0638
9.310	213.605	12.524	0.0670	0.1	0.0669
10.069	214.274	13.287	0.0697	0.5	0.0697
11.106	214.386	14.251	0.0735	0.8	0.0735
12.419	214.475	15.168	0.0776	1.0	0.0777
14.257	215.019	16.048	0.0819	0.6	0.0819
16.765	215.367	16.982	0.0873	0.4	0.0873
20.273	215.152	18.017	0.0944	0.1	0.0944
24.888	215.458	18.965	0.1021	−0.1	0.1020
31.249	215.191	19.996	0.1116	−0.3	0.1115
39.616	214.914	21.015	0.1223	−0.5	0.1223
48.551	215.174	21.833	0.1323	−0.4	0.1323
57.649	215.416	22.520	0.1415	−0.3	0.1414
66.102	215.167	23.093	0.1499	0.0	0.1499
69.271	215.146	23.285	0.1531	0.3	0.1552
		Nom. temp. 235			
0.978	234.032	0.523	0.0264	0.2	0.0265
3.146	235.091	1.849	0.0294	−0.5	0.0294
5.136	234.443	3.371	0.0336	0.6	0.0336
7.132	234.917	5.260	0.0394	0.4	0.0395
9.427	233.946	8.134	0.0504	−0.1	0.0504
11.472	234.177	10.553	0.0592	−0.4	0.0592
13.602	234.489	12.421	0.0662	0.2	0.0662
15.751	234.368	13.834	0.0723	0.9	0.0723
17.693	234.156	14.822	0.0770	1.0	0.0770
20.535	233.996	15.927	0.0828	0.9	0.0829
23.411	234.454	16.735	0.0878	0.8	0.0879
26.932	234.323	17.591	0.0936	0.4	0.0936
30.364	234.387	18.260	0.0990	0.6	0.0991
34.090	234.158	18.897	0.1036	−0.2	0.1037
37.547	234.589	19.362	0.1080	−0.2	0.1080
41.020	234.483	19.814	0.1123	−0.3	0.1123
44.352	234.423	20.202	0.1164	−0.1	0.1165

Table II. *(Continued)*

Pressure (MPa)	Temperature (%)	Density (mol·L^{-1})	Thermal conductivities: Experimental (W·m^{-1}·K^{-1})	Exp. − corr. (%)	At nom. T (W·m^{-1}·K^{-1})
47.930	234.300	20.585	0.1203	−0.2	0.1204
51.243	234.276	20.905	0.1240	−0.0	0.1241
55.102	234.676	21.225	0.1278	−0.0	0.1278
58.416	234.636	21.502	0.1311	−0.0	0.1311
61.886	234.566	21.775	0.1344	−0.0	0.1345
65.384	234.491	22.034	0.1379	0.2	0.1380
68.759	234.492	22.267	0.1412	0.4	0.1432
		Nom. temp. 255			
1.019	254.900	0.497	0.0289	0.6	0.0289
2.715	255.589	1.394	0.0308	0.0	0.0308
4.725	254.985	2.609	0.0337	0.2	0.0337
6.554	254.668	3.877	0.0371	0.7	0.0371
6.789	255.612	4.019	0.0377	0.9	0.0376
8.786	254.994	5.610	0.0428	1.7	0.0428
11.185	255.303	7.640	0.0494	0.1	0.0494
13.271	254.923	9.413	0.0556	−0.8	0.0556
15.399	255.348	10.900	0.0612	−0.3	0.0612
17.521	255.114	12.182	0.0663	0.1	0.0663
20.353	254.901	13.541	0.0724	0.6	0.0724
23.423	255.262	14.644	0.0778	0.7	0.0778
26.850	254.972	15.688	0.0834	0.5	0.0834
30.399	254.910	16.551	0.0888	0.4	0.0888
33.908	254.840	17.267	0.0937	0.3	0.0937
37.374	254.834	17.873	0.0981	0.2	0.0981
40.729	255.712	18.329	0.1022	0.4	0.1021
44.632	255.337	18.887	0.1063	−0.2	0.1063
48.089	255.228	19.317	0.1102	−0.2	0.1101
51.673	255.159	19.720	0.1139	−0.3	0.1139
56.207	255.275	20.172	0.1184	−0.3	0.1184
59.686	254.844	20.517	0.1221	−0.2	0.1221
63.257	255.191	20.807	0.1256	0.1	0.1256
66.476	255.135	21.071	0.1287	0.2	0.1308
		Nom. temp. 275			
1.015	274.936	0.455	0.0314	0.6	0.0314
2.496	275.113	1.160	0.0328	0.2	0.0328

Table II. *(Continued)*

Pressure (MPa)	Temperature (K)	Density ($mol \cdot L^{-1}$)	Thermal conductivities: Experimental ($W \cdot m^{-1} \cdot K^{-1}$)	Exp. − corr. (%)	At nom. T ($W \cdot m^{-1} \cdot K^{-1}$)
4.448	274.767	2.174	0.0350	0.1	0.0350
6.507	274.636	3.350	0.0381	1.0	0.0381
8.404	276.448	4.465	0.0413	1.0	0.0411
10.555	275.848	5.876	0.0455	1.0	0.0454
12.675	275.900	7.277	0.0501	0.6	0.0500
14.654	276.042	8.536	0.0545	0.2	0.0544
16.955	275.731	9.909	0.0594	0.0	0.0593
19.154	275.513	11.057	0.0637	0.1	0.0637
21.325	275.548	12.020	0.0677	0.3	0.0676
23.532	275.376	12.887	0.0715	0.4	0.0715
26.986	275.171	14.031	0.0770	0.7	0.0770
30.488	275.086	14.986	0.0821	0.6	0.0821
33.989	275.696	15.746	0.0868	0.8	0.0867
37.530	275.223	16.482	0.0901	−0.7	0.0901
41.152	275.114	17.118	0.0955	0.4	0.0954
44.660	275.014	17.664	0.0995	0.4	0.0995
48.079	274.960	18.141	0.1030	0.1	0.1030
51.733	275.416	18.576	0.1066	0.1	0.1066
55.235	275.391	18.981	0.1102	0.1	0.1101
58.748	275.294	19.359	0.1136	0.1	0.1135
62.501	275.235	19.731	0.1172	0.2	0.1171
65.837	275.175	20.039	0.1201	0.2	0.1201
69.253	275.654	20.311	0.1231	0.4	0.1252
		Nom. temp. 295			
0.988	295.744	0.409	0.0338	−0.6	0.0337
1.949	295.507	0.823	0.0346	−0.6	0.0346
3.913	295.202	1.716	0.0364	−0.7	0.0364
5.978	295.471	2.717	0.0387	−0.6	0.0387
8.081	294.956	3.811	0.0415	0.0	0.0415
10.369	294.539	5.060	0.0450	0.4	0.0451
12.173	294.243	6.070	0.0481	0.6	0.0482
14.298	294.691	7.218	0.0517	0.1	0.0517
16.381	294.370	8.334	0.0553	−0.4	0.0554
18.660	294.082	9.468	0.0594	−0.5	0.0595
21.433	293.899	10.692	0.0641	−0.3	0.0642
25.128	294.496	12.024	0.0696	−0.3	0.0697
28.716	294.508	13.136	0.0748	−0.0	0.0749

Table II. *(Continued)*

Pressure (MPa)	Temperature (K)	Density ($mol \cdot L^{-1}$)	Thermal conductivities: Experimental ($W \cdot m^{-1} \cdot K^{-1}$)	Thermal conductivities: Exp. – corr. (%)	Thermal conductivities: At nom. T ($W \cdot m^{-1} \cdot K^{-1}$)
32.485	295.407	14.068	0.0794	−0.2	0.0793
36.136	295.265	14.905	0.0837	−0.4	0.0837
39.443	295.194	15.569	0.0875	−0.5	0.0875
42.827	295.160	16.174	0.0912	−0.5	0.0912
46.333	295.074	16.742	0.0950	−0.6	0.0949
50.000	295.067	17.274	0.0988	−0.5	0.0988
53.683	294.925	17.767	0.1023	−0.6	0.1023
57.061	294.439	18.200	0.1056	−0.5	0.1057
60.577	294.387	18.596	0.1089	−0.4	0.1090
63.953	294.307	18.951	0.1120	−0.2	0.1121
67.321	294.908	19.251	0.1150	−0.0	0.1169
		Nom. temp. 310			
1.076	308.077	0.428	0.0358	−0.3	0.0362
2.676	308.321	1.090	0.0372	−0.5	0.0374
4.743	308.535	1.992	0.0392	−0.3	0.0394
6.733	308.770	2.904	0.0414	0.2	0.0416
8.877	308.465	3.938	0.0441	0.6	0.0443
11.039	308.457	5.004	0.0470	0.9	0.0473
13.148	308.190	6.060	0.0502	1.0	0.0504
15.186	307.983	7.066	0.0532	0.7	0.0535
17.278	308.627	8.021	0.0564	0.3	0.0566
19.464	308.425	8.996	0.0599	0.2	0.0601
22.419	308.247	10.192	0.0642	−0.1	0.0644
26.028	308.149	11.459	0.0694	0.0	0.0697
29.477	308.931	12.448	0.0741	0.4	0.0743
33.098	308.562	13.413	0.0783	−0.0	0.0786
36.520	308.422	14.202	0.0821	−0.3	0.0824
39.911	308.215	14.903	0.0861	−0.1	0.0864
43.082	308.821	15.451	0.0893	−0.2	0.0895
46.727	308.702	16.063	0.0931	−0.1	0.0933
50.126	308.620	16.581	0.0964	−0.2	0.0967
53.476	308.585	17.047	0.0997	−0.1	0.0999
57.009	308.454	17.505	0.1030	0.0	0.1033
60.531	308.395	17.924	0.1063	0.2	0.1066
64.078	308.364	18.315	0.1093	0.2	0.1096
66.676	312.206	18.414	0.1106	0.2	0.1103
67.415	308.467	18.653	0.1125	0.6	0.1127

densities. The dependence of thermal conductivity on temperature and density is normally expressed as

$$\lambda(\rho, T) = \lambda_0(T) + \lambda_{\text{excess}}(\rho, T) + \Delta\lambda_{\text{critical}}(\rho, T) \tag{1}$$

The first term on the right in Eq. (1) is the dilute gas term, which is independent of density. The second is the excess thermal conductivity. The first two terms taken together are sometimes called the "background" thermal conductivity. The final term is the critical-point enhancement. The various terms used in the correlation are shown schematically in Fig. 2.

4.1. Term 1, the Dilute Gas

To obtain a value at zero density from the experiment we must extrapolate the measurements at low densities to zero density, usually with a low-order polynomial. This was done with the experimental values after they had been adjusted slightly to even values of temperature. The extrapolations for 13 isotherms are given in Table III. They are compared

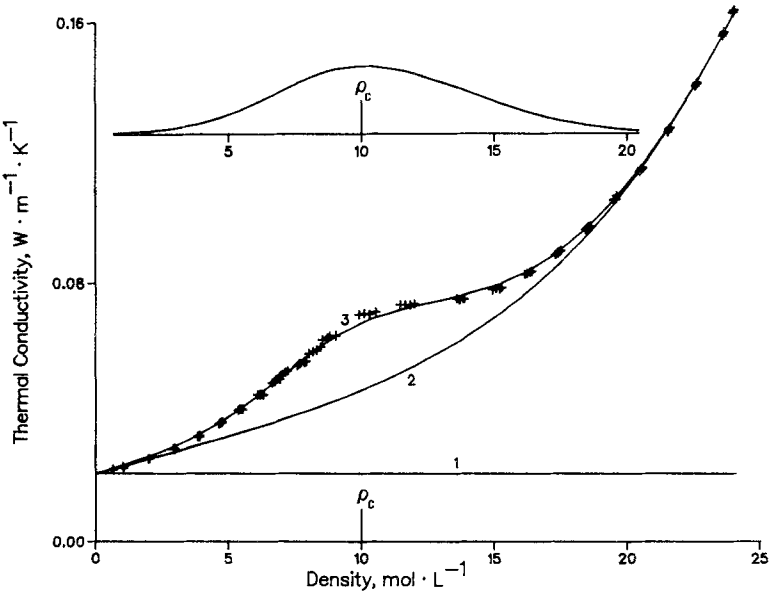

Fig. 2. Isotherm analysis illustrated for a temperature of 197 K. (+) Experimental points. (1) The dilute gas term, λ_0; (2) the background conductivity, $\lambda_0 + \lambda_{\text{excess}}$; (3) the calculated thermal conductivity. Inset: $\Delta\lambda_{\text{critical}}$.

Table III. Extrapolated and Calculated Dilute Gas Thermal Conductivites, λ_0

Temperature (K)	Maximum density ($mol \cdot L^{-1}$)	Dilute gas thermal conductivity (λ)					
		Extrapolated		Calc. (Sect. 4.5)		Calc. (Ref. 4)	
		($W \cdot m^{-1} \cdot K^{-1}$)	($\pm 2\sigma$)	($W \cdot m^{-1} \cdot K^{-1}$)	(%)	($W \cdot m^{-1} \cdot K^{-1}$)	(%)
133.0		0.01392		0.01386		0.01495	
143.0	0.620	0.01497	0.00011	0.01505	−0.55	0.01609	−7.48
155.0	1.029	0.01640	0.00031	0.01644	−0.26	0.01746	−6.44
163.0	1.603	0.01733	0.00012	0.01735	−0.13	0.01836	−5.95
175.0	2.538	0.01870	0.00025	0.01870	−0.02	0.01971	−5.41
183.0	2.713	0.01962	0.00050	0.01961	0.03	0.02060	−5.02
197.0	2.972	0.02131	0.00033	0.02115	0.77	0.02218	−4.07
215.0	3.144	0.02312	0.00023	0.02305	0.31	0.02422	−4.75
235.0	3.392	0.02560	0.00007	0.02529	1.19	0.02654	−3.69
255.0	5.539	0.02803	0.00008	0.02768	1.27	0.02894	−3.24
275.0	4.495	0.03054	0.00012	0.03025	0.93	0.03143	−2.92
295.0	3.832	0.03301	0.00008	0.03308	−0.22	0.03403	−3.09
310.0	3.953	0.03536	0.00016	0.03540	−0.12	0.03605	−1.95

with values for the dilute gas at zero density obtained by Hanley et al. [4] in both Table III and Fig. 3. The differences are seen to be nearly constant at 0.001 $W \cdot m^{-1} \cdot K^{-1}$. A simple cubic polynomial is sufficient to represent the experimental values of λ_0 as a function of temperature:

$$\lambda_0(T) = A_1 + A_2 T + A_3 T^2 + A_4 T^3 \tag{2}$$

where the coefficients were determined in the single surface fit (Section 4.4).

$$A_1 = -0.886333344 \times 10^{-2}$$

$$A_2 = 0.2419639784 \times 10^{-3}$$

$$A_3 = -0.6997019196 \times 10^{-6}$$

$$A_4 = 0.1224609018 \times 10^{-8}$$

with λ_0 in $W \cdot m^{-1} \cdot K^{-1}$ and T in K.

4.2. Term 2, the Excess Thermal Conductivity

The use of an exponential in term 2 has been extensive; see, for example, Refs. 4–10. However, the use of a fractional exponent on density has

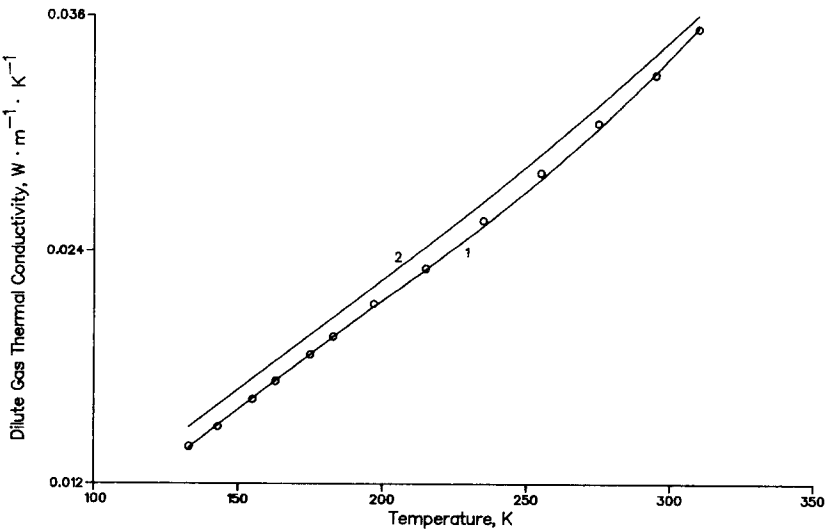

Fig. 3. The dilute gas thermal conductivity, λ_0, of methane. (○) Extrapolation of present measurements. (1) This paper; (2) Ref. 4.

recently been called to question [15] because it may give rise to an infinite $d\lambda/d\rho$ near zero density. The expression used in Refs. 5–10 for the excess thermal conductivity was

$$\lambda_{\text{excess}}(\rho, T) = \alpha\rho + \delta[e^{\beta\rho^7} - 1.0]$$

Rather than to try to compensate for the inherent problem in the exponential term, we substitute a simpler term, $\beta\rho^n$, for the exponential. The exponent n has a value between 3 and 4. The functional form becomes

$$\lambda_{\text{excess}}(\rho, T) = \alpha\rho + \beta\rho^n$$

Initial estimates for the term $\alpha\rho$ for each isotherm are determined from the values at the three lowest density levels, about 12 points. Similarly, initial estimates for the term $\beta\rho^n$ are determined from the six highest density levels, about 24 points. These initial estimates show that α, β, and n are functions of temperature. The coefficients α and n can be represented by low-order polynomials in temperature. Since β varies through an order of magnitude, it turns out that $\log(\beta)$ is amenable to fitting as a cubic in temperature. The complete expression for the excess thermal conductivity as used for methane is

$$\lambda_{\text{excess}}(\rho, T) = (B_1 + B_2)\rho + e^{(B_3 + B_4 T + B_5 T^2 + B_6 T^3)} \rho^{(B_7 + B_8 T + B_9 T^2)} \qquad (3)$$

The coefficients were determined in a single surface fit (Section 4.4).

$$B_1 = 0.2773027550 \times 10^{-}2$$
$$B_2 = -0.2477683184 \times 10^{-5}$$
$$B_3 = -0.1458682198 \times 10^{-2}$$
$$B_4 = -0.1982760371 \times 10^{-1}$$
$$B_5 = 0.1009665010 \times 10^{-3}$$
$$B_6 = -0.2595460306 \times 10^{-7}$$
$$B_7 = 0.3691505315 \times 10^{+1}$$
$$B_8 = 0.6857505926 \times 10^{-2}$$
$$B_9 = -0.3009401784 \times 10^{-4}$$

with λ_{excess} in $\text{W} \cdot \text{m}^{-1} \cdot \text{K}^{-1}$, ρ in $\text{mol} \cdot \text{L}^{-1}$, and T in K.

4.3. Term 3, the Critical Enhancement

With the background thermal conductivity determined, we turn our attention to the critical enhancement. We subtract Eqs. (2) and (3) from the experimental values to obtain a remainder which is essentially the critical enhancement. The remainders are plotted in Fig. 4. In the analysis on oxygen [8] we considered two separate regions, the critical region

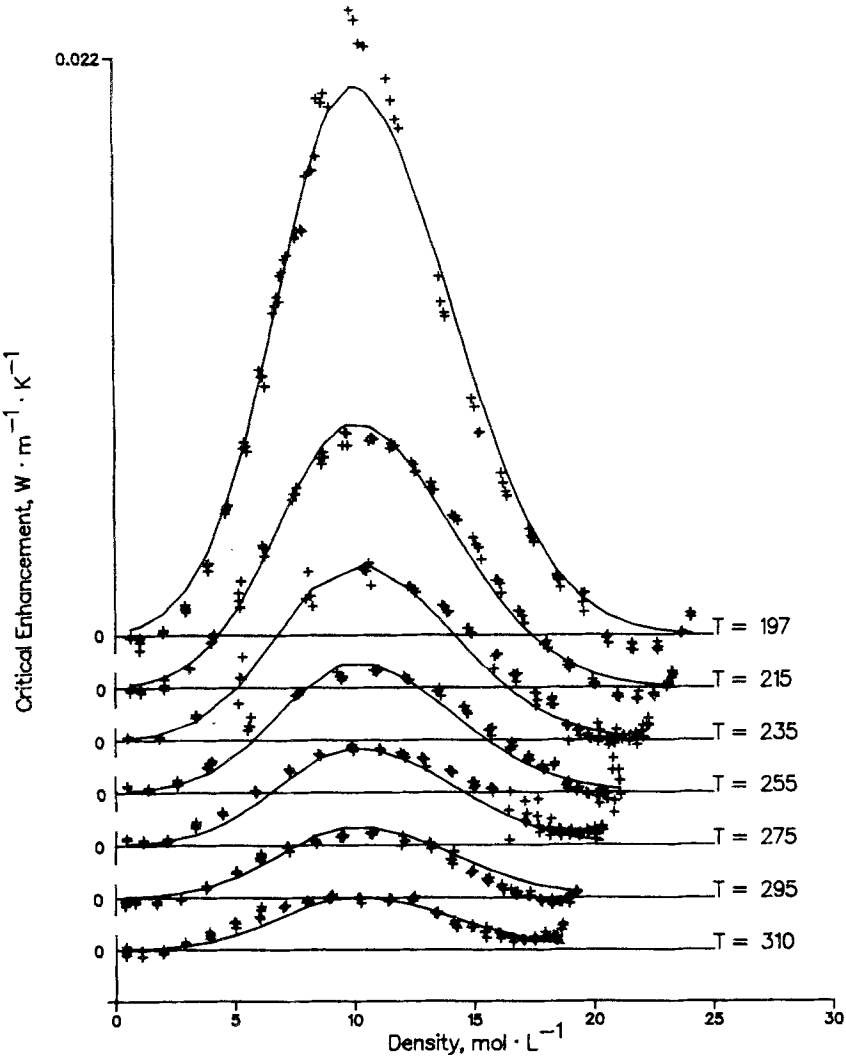

Fig. 4. The critical enhancement for methane along isotherms. Isotherms are separated by 0.002 $W \cdot m^{-1} \cdot K^{-1}$.

proper and the extended critical region. For the critical region proper we recommend the use of the scaled equation of state developed by Sengers et al. [16]. For methane, $T_c = 190.555$ K and $\rho_c = 10.0$ mol · L^{-1}. The corresponding boundaries of the critical region proper are $185 \leqslant T \leqslant 196$ K and $7.5 \leqslant \rho \leqslant 12.5$ mol · L^{-1}.

For methane all of the measurements fall into the extended critical region. To represent the remainders shown in Fig. 4 we use the function, e^{-x^2}, quite similar to the analysis on oxygen [8], shown schematically in the inset in Fig. 2. The variable x is a simple function of density chosen to be zero at the maximum value of the critical enhancement, i.e., at a density of ρ_c.

$$x = C(\rho - \rho_c) \tag{4}$$

The small asymmetry seen in Fig. 4 is achieved by providing different coefficients in Eq. (4) above and below the critical density as follows:

$$x = C_5(\rho - \rho_c) \quad \text{for } \rho < \rho_c \qquad \text{and} \qquad x = C_6(\rho - \rho_c) \quad \text{for } \rho > \rho_c.$$

The maximum value of $\Delta\lambda_c$ is the amplitude (AMPL) of the function for the particular temperature under consideration. The amplitude is chosen to be a simple function of temperature as follows:

$$\text{AMPL} = C_1/(T + C_2) + C_3 + C_4 T$$

The complete expression for the critical enhancement in the extended critical region becomes

$$\Delta\lambda_{\text{critical}}(\rho, T) = \text{AMPL}\, e^{-x^2}$$

or

$$\Delta\lambda_{\text{critical}}(\rho, T) = \left(\frac{C_1}{T + C_2} + C_3 + C_4 T\right) e^{-[C_5(\rho - \rho_c)]^2} \quad \text{for } \rho < \rho_c \tag{5a}$$

and

$$\Delta\lambda_{\text{critical}}(\rho, T) = \left(\frac{C_1}{T + C_2} + C_3 + C_4 T\right) e^{-[C_6(\rho - \rho_c)]^2} \quad \text{for } \rho < \rho_c \tag{5b}$$

where the coefficients were determined in a single surface fit (Section 4.4).

$$C_1 = 0.20594937228$$

$$C_2 = -185.0$$

$$C_3 = 0.9517540680 \times 10^{-2}$$

$$C_4 = -0.2944481220 \times 10^{-4}$$

$$C_5 = -0.2244399588$$

$$C_6 = 0.1720710404$$

with $\Delta\lambda_{\text{critical}}$ in $W \cdot m^{-1} \cdot K^{-1}$, ρ in $mol \cdot L^{-1}$, and T in K.

4.4. The Thermal Conductivity Surface

Equations (1), (2), (3), and (5) describe the thermal conductivity surface of methane in the region of the present measurements. Not implemented in the present correlation is the critical region proper. For conditions close to the critical point we recommend the formulation of Sengers et al. [16]. Coefficients for Eqs. (2), (3), and (5) were determined by running alternate cycles of a linear last-squares routine on nine of the coefficients and one parameter and then a general minimizing routine on the remaining nine parameters until the change in the total deviation sum became negligible. Since the variables normally available to the user are pressure and temperature, an equation of state [12] is required to find the density corresponding to an input pressure. Temperature and density then allow calculation of the thermal conductivity from the functions given.

Deviations between experimental values and the calculated surface are shown for all points in Fig. 5 by isotherms. The average percentage deviation for all 900 points is 0.6%; this is equivalent to 1.6% at the 2σ level.

5. DISCUSSION

The precision of the measurements can be established from several considerations. These are the linear regression statistics for a thermal conductivity point, the variation in the measured thermal conductivity with the applied power, and the variation obtained in a curve fit of the thermal conductivity along an isotherm. The precision of the measurements as established by varying the applied power is 0.6% [5, 6]. The reproducibility of the present measurements as seen in Fig. 5 is about 1.6% for the worst case at a temperature of 197 K.

The accuracy of the apparatus can be established, in principle, from

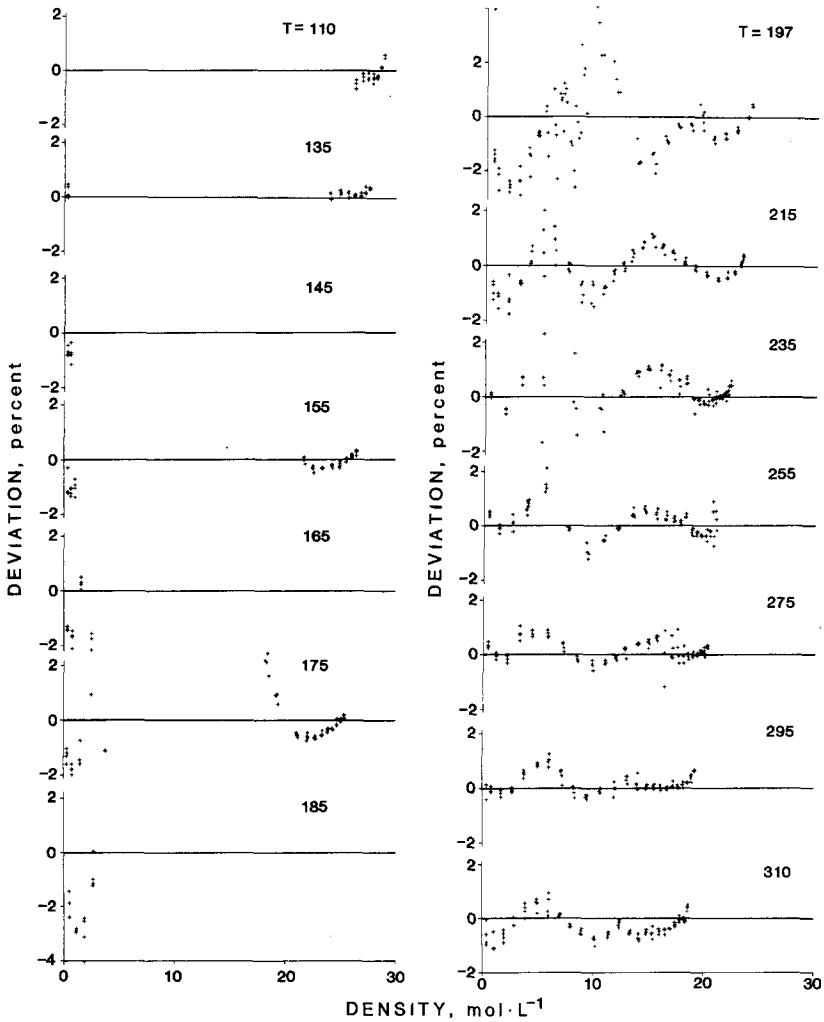

Fig. 5. Deviations of the experimental points from the correlation along isotherms.

measurements on the rare gases and certain theoretical considerations, i.e., the Eucken factor [6, 7]. For the present results the accuracy was estimated from the variation obtain in the curve fit of the thermal conductivity surface considering different densities and different temperatures. This estimate of accuracy is 1.6% (2σ).

Comparisons with the results of others who used different systems [1, 2] and who used a transient hot wire [3] also yield an estimate of

accuracy. The comparisons were made through the present correlating surface at several temperatures and are plotted in Figs. 6–8. Near 300 K the agreement between the results of Le Neindre et al. [2] and the present results is better than 1.3% over the entire range of overlap in pressure. This agreement is truly excellent considering that we are comparing the very lowest temperature of [2] with the very highest temperature in the present measurements. Le Neindre's results go to densities beyond 20 mol · L^{-1}, and we see from Fig. 6 that extrapolation of the present correlating surface beyond the densities of the measurement is not warranted. The agreement between the results of Mani [3] and the present measurements is better than 1.8% for all of Mani's measurements for which the density is greater than critical density. The agreement is well within the combined uncertainties. For Mani's measurements at densities lower than critical, we assume that the lack of end-effect compensation coupled with the extrapolation to zero time produced inaccurate results. In Fig. 7 at a temperature of 240 K, the agreement between the present results and those of Mani [3] is better than 1%. At this temperature the agreement between the highest isotherm of Sokolova and Golubev [1] and the present results is about 4% over the entire range of densities, not outstanding but acceptable. In Fig. 8 the lowest temperature of comparison, 210 K, the results of Mani [3] and the

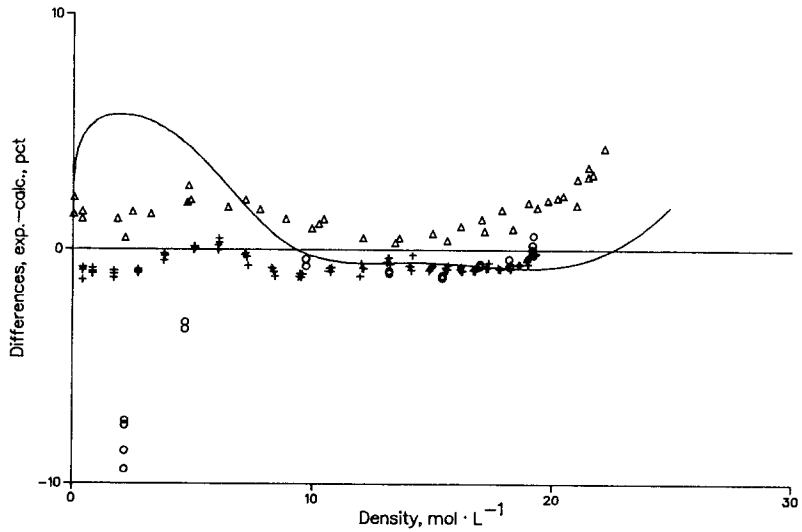

Fig. 6. Comparison of the present correlation with the results of others near 300 K. (+) Present measurements, 295 K; (△) Ref. 2, 300 K; (○) Ref. 3, 300 K; (——) the correlation of Ref. 4.

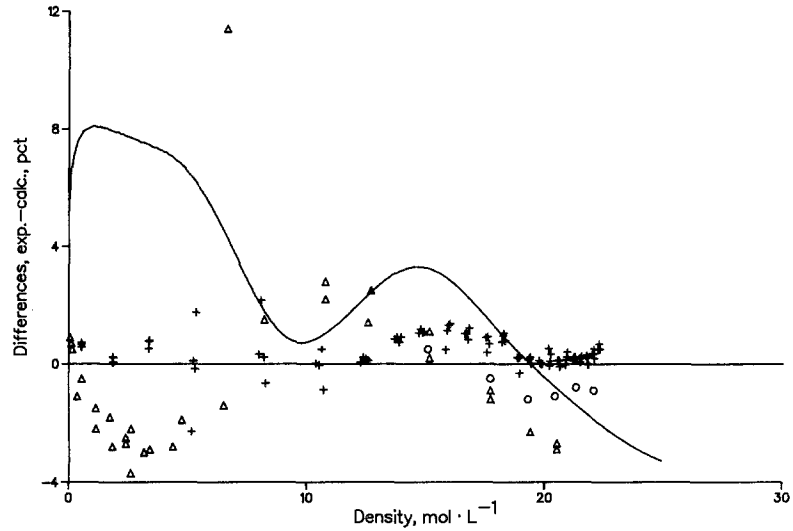

Fig. 7. Comparison of the present correlation with the results of others near 240 K. (+) Present measurements, 235 K; (△) Ref. 1, 235 K; (○) Ref. 3, 240 K; (——) the correlation of Ref. 4.

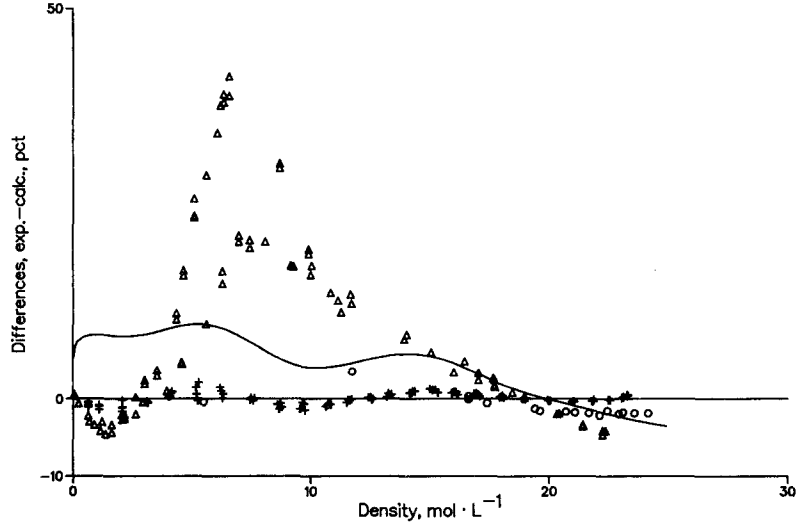

Fig. 8. Comparison of the present correlation with the results of others near 210 K. (+) Present measurements, 215 K; (△) Ref. 1, 210 and 216 K; (○) Ref. 3, 200 and 220 K; (——) the correlation of Ref. 4.

present results agree to better than 2% over the entire range of densities. For Sokolova and Golubev we observe that the agreement is still about 4% for densities between 0 and 3 mol · L^{-1} and also above 17 mol · L^{-1}, however, for densities in between the departures become large. Since the maximum departures fall considerably below critical density, we conclude that Sokolova and Golubev had a sizable convection component in their experiment.

The present measurements show the thermal conductivity surface of methane to be very similar to that of oxygen [8]. The present correlation is based on the description developed for oxygen but there are several major differences. First, there is the use of the term $\beta\rho^n$ rather than an exponential. Second, the center density of the critical enhancement does not appear to be a function of temperature as in oxygen. For methane the use of ρ_c as the centering density seems to suffice. Third, the critical enhancement above and below critical density is decidedly unsymmetric. The last probably results from the term $\beta\rho^n$. There are several drawbacks to the abbreviated correlation presented here. Extrapolation to densities or temperatures higher than those experimentally measured does not seem to be warranted. The scaling laws describing the critical region proper [16] have not been implemented here. Finally, the analysis of the critical enhancement at temperatures below critical is incomplete. For oxygen it was noted that the experimental $\Delta\lambda_{\text{critical}}$ for temperatures below critical was larger than that calculated for an equivalent point above the critical temperature. For methane a sufficient number of isotherms below critical temperature have been measured, however, a detailed analysis of the critical enhancement for temperatures below critical remains to be completed.

The new data are compared through the present correlation to a previous one by Hanley et al. [4] in Figs. 6–8. Systematic deviations between the older correlation and the experimental values are seen for the dilute gas and at the lower densities. Maximum deviations occur at about 3 mol · L^{-1} and are probably caused by the use of the exponential term in the excess thermal conductivity of [4]. At 215 K the older correlation is in error by 10% for all densities up to 15 mol · L^{-1}. The average deviation produced by the older correlation for all 900 new experimental points is 3.3%.

6. SUMMARY

The thermal conductivity of methane has been measured at temperatures from 110 to 310 K with pressures to 70 MPa. The measurements cover the physical states of the dilute gas, the dense gas, the region near critical, compressed liquid states, metastable liquid states at conditions just

below saturation, and vapor states at temperatures below critical and pressures less than the vapor pressure. The results were analyzed in conventional terms to develop an interim description of the thermal conductivity surface. The new surface reveals that the critical enhancement persists to the highest temperatures measured here, 310 K. The enhancement is asymmetric about its center density. The accuracy of the present measurements is 1.6% (2σ) as established from the fit of the correlating surface and by comparison with the very best results of others. In view of the new masurements and in view of the defects in both the present and the older correlation, we suggest that further work on the conductivity correlation of methane is called for.

ACKNOWLEDGMENT

The author would like to express his appreciation to B. Segal for his assistance in making the experimental masurements.

REFERENCES

1. V. P. Sokolova and I. F. Golubev, *Teploenergetika* **14**:91 (1967).
2. B. Le Neindre, R. Tufeu, and P. Bury, *Proc. Int. Therm. Cond. Conf. 8th*, C. Y. Ho, et al., eds. (Plenum Press, New York, 1969), p. 75.
3. N. Mani, Thesis University of Calgary, Calgary, Alberta, Canada, 1971).
4. H. J. M. Hanley, W. M. Haynes, and R. D. McCarty, *J. Phys. Chem. Ref. Data* **6**:597 (1977).
5. H. M. Roder, *J. Res. Natl. Bur. Stand. (U.S.)* **86**:457 (1981).
6. C. A. N. de Castro and H. M. Roder, *J. Res. Natl. Bur. Stand. (U.S.)* **86**:293 (1981).
7. C. A. N. de Castro and H. M. Roder, *Proc. 8th Symp. Thermophys. Prop.*, J. V. Sengers, ed. (ASME, New York, 1982), p. 241.
8. H. M. Roder, *J. Res. Natl. Bur. Stand. (U.S.)* **87**:279 (1982).
9. H. M. Roder and C. A. N. de Castro, *J. Chem. Eng. Data* **27**:12 (1982).
10. H. M. Roder, *Proc. Int. Therm. Cond. Conf. 17th*, J. G. Hust, ed. (Plenum, New York, 1983), p. 257; H. M. Roder, *Int. J. Thermophys* **5**:323 (1984).
11. T. Bruno, Private communication, this laboratory.
12. R. D. McCarty, Natl. Bur. Stand. (U.S.) Technical Note 1025 (1980).
13. H. M. Roder, Natl. Bur. Stand. (U.S.), NBSIR 84-3006 (1984).
14. D. E. Diller, H. J. M. Hanley, and H. M. Roder, *Cryogenics* **10**:286 (1970).
15. D. G. Friend and J. C. Rainwater, Private communication, this laboratory.
16. J. V. Sengers, R. S. Basu, and J. M. H. Levelt Sengers, NASA Contractor Report 3424 (NASA Scientific and Technical Information Branch, 1981), p. 59.